Electronic Supplementary Material (ESI) for Dalton Transactions.

Electronic Supplementary Information

Increasing the Stability of Calixarene-Capped Porous Cages Through Coordination Sphere Tuning

Avishek Dey,[†] Michael R. Dworzak,[†] Kaushalya D. P. Korathotage,[‡] Munmun Ghosh,[†] Jahidul Hoq,[‡] Christine M. Montone,[‡] Glenn P. A. Yap,[†] and Eric D. Bloch*[†,‡]

[†]Department of Chemistry and Biochemistry, University of Delaware, Newark, Delaware 19716, United States

[‡]Department of Chemistry, Indiana University, Bloomington, Indiana 47405, United States

List of Contents

Materials

All reagents and solvents were purchased from commercial sources and used without further purification. Syntheses of triazole ligands, sulfonylcalix[4]arenes (sc4a), Fe and Co-containing cages were carried out using standard Hood, Schlenk and glovebox techniques unless otherwise specified. Specified solvents were purchased from Sigma-Aldrich and stored in a glovebox over molecular sieves prior to use. All other solvents were deoxygenated by thoroughly sparging with Ar and dried on a solvent purification system (SPS) by SG Water, USA LLC. Solvents were stored in a glovebox over molecular sieves once removed from the SPS. The sulfonylcalix[4]arene ligand (sc4a), and triazole ligands were synthesized with minor modifications from previously reported synthetic protocols.

Gas Adsorption Measurements

Low-pressure gas adsorption measurements were obtained on a Micromeritics Tristar II PLUS, a Micromeritics Tristar 3000. Following DMF and MeOH exchange, solvent was decanted, and residual solvent was removed to obtain cage materials as free-flowing powders. Samples were activated under vacuum at a temperature optimized for each material using a Micromeritics Tristar flow station and for PC-1(Fe)box Micromeritics 3Flex Degas Station was used overnight.

IR Spectroscopy

IR spectra were obtained on a Bruker ALPHA II ATR-IR spectrometer with OPUS data processing software. Most of the samples were measured in air and box samples were transferred from an inert atmosphere glovebox immediately prior to measurements, which were carried out in air.

Thermogravimetric Analysis

Thermogravimetric analysis measurements were obtained using a TA Q5000 SA under N_2 flow. Most of the samples were measured in air and box made samples were transferred from an inert atmosphere glovebox immediately prior to measurements, which were carried out in air. During the measurements, samples were heated from room temperature to 600 °C at a rate of 2-5 °C per minute.

Powder X-Ray Diffraction Measurements

Powder X-Ray diffraction measurements were obtained at the University of Delaware Advanced Materials Characterization Laboratory using a Bruker D8 X-ray diffractometer with a LynxEye detector and Cu Kα radiation (λ = 1.54 Å).

Synthetic Procedures

Synthesis of p-tert-Butylthiacalix[4]arene (TC4A).[1] To a 1 L round-bottom flask, p-tert-butylphenol (64.5 g, 0.43 mol), elemental sulfur (27.5 g, 0.86 mol), NaOH (8.86 g, 0.215 mol), and tetraethylene gylcol dimethyl ether (19 mL) were added and stirred under a flow of nitrogen. The mixture was heated to 230 °C over 4 h and held at this temperature overnight. The mixture was allowed to cool to room temperature, yielding a dark-brown solid to which toluene (35 mL) and 4 M H_2SO4 (78 mL) were added. The flask was then sonicated for 30 min, and the solubilized material was transferred to a separatory funnel. The organic phase was collected, and MeOH (400 mL) was added, precipitating the product as a light-brown powder that could be isolated by vacuum filtration. This process was repeated until all of the initially generated solid was dissolved. The collected product was dried for 24 h prior to use.

Synthesis of p-tert-Butylsulfonylcalix[4]arene (SC4A).[2] In a 1 L round-bottom flask, TC4A (7 g, 46.7 mmol) and sodium perborate tetrahydrate (14 g, 91.0 mmol) were added to a mixture of chloroform (210 mL) and acetic acid (350 mL). The resultant solution was heated with stirring at 50 °C for 18 h. After the solution cooled to room temperature, H_2O (300 mL) was added, and the solution was transferred to a separatory funnel. The organic layer was collected, and the solvent was removed via rotary evaporation before an excess of Et_2O was added; the precipitated white solid was collected via vacuum filtration. The product was dried for 24 h prior to use.

Synthesis of 1,3,5-tris[1*H* 1,2,3-triazol-5-yl]benzene (H_3BTTri)[3]

To 50 mL of tetrahydrofuran was added 35 mL of formaldehyde (37 wt% in H_2O) and 4.05 mL of acetic acid, and this mixture was stirred at room temperature for 15 min. Sodium azide (4.58 g) was then added slowly, followed by 1,3,5-triethynylbenzene (2.36 g). The mixture was stirred at room temperature for another 10 min, after which sodium ascorbate (1.86 g) and a solution of 1.25 M aqueous copper sulfate (2 mL) were added. After stirring at room temperature for 48h, the reaction was diluted with water and the product was filtered and washed with more water. To deprotect the triazole groups, the product was redissolved in 3:1 MeOH:2M NaOH mixture and stirred at room temperature for 48 h. During this process, copper hydroxide crashed out as a blue/green solid. The blue precipitate was allowed to settle, and then filtered out and discarded. The filtrate was then neutralized with acetic acid. The white solid that precipitated out was then filtered, washed with water, and dried to give 3.5 g of ligand.

Synthesis of 1,3-bis(1*H* 1,2,3-triazol-5-yl)benzene (H_2BDTri)[3]

To 40 mL of tetrahydrofuran was added 11.66 mL of formaldehyde (37 wt% in H_2O) and 2.7 mL of acetic acid, and this mixture was stirred at room temperature for 15 min. Sodium azide (3.10 g) was then added slowly, followed by 1,3-triethynylbenzene (2 g). The

mixture was stirred at room temperature for another 10 min, after which sodium ascorbate (1.254 g) and a solution of 0.1 equiv aqueous copper sulfate (394 mg in 1 mL H_2O) were added. After stirring at room temperature for 48h, the reaction was diluted with water and the product was filtered and washed with more water. To deprotect the triazole groups, the product was redissolved in 3:1 MeOH:2M NaOH mixture and stirred at room temperature for 48 h. During this process, copper hydroxide crashed out as a blue/green solid. The blue precipitate was allowed to settle, and then filtered out and discarded. The filtrate was then neutralized with acetic acid. Further, the mixture was added to the excess amount of water for 24h. The white solid that precipitated out was then filtered, washed with water, and dried to give ligand.

Synthesis of $[(Fe_4OHsc4a)_6(BTTri)_8]^{6-}$

To a 20 ml vial, H_3BTTri (48 mg) was dissolved in 6 ml DMF 120 °C for 1h. Dimethylformamidium was cooled to room temperature and diluted to a 2 ml EtOH solution. This mixture was heated at 120 °C until product precipitating as orange crystalline product. The crystalline product was isolated by decanting the supernatant solution, rinsed with DMF, and soaked in 3 mL of DMF at 120 °C for 2 h. Subsequently, the solids were exchanged with MeOH over 2 d, with the solvent replenished with every day. MeOH was decanted and materials were evacuated at room temperature to give orange crystalline powders. Samples for gas adsorption were subsequently evacuated at 150 °C overnight using Micromeritics Tristar flow station.

Synthesis of $[(Co_4OHsc4a)_6(BTTri)_8]^{6-}$

To a 20 ml vial, H_3BTTri (48 mg) was dissolved in 6 ml DMF 120 °C for 1h. Dimethylformamidium trifluoromethanesulfonate (96 mg) and $CoCl_2$. $6H_2O$ (30mg) was added to that solution. The mixture was heated at 120 °C for 3h. After cooling to room temperature, sc4a (68 mg) was added to that mixture. Further, MeOH (2 ml) was added to the mixture and the solution was heated for an additional 48 h at 120 °C. The resultant solution was cooled to room temperature and diluted to a 2 ml EtOH solution. This mixture was heated another 120 °C until product precipitating as pink crystalline product. The crystalline product was isolated by decanting the supernatant solution, rinsed with DMF, and soaked in 5 mL of DMF overnight. Subsequently, the solids were exchanged with MeOH over 2 d, with the solvent replenished with every day. MeOH was decanted and materials were evacuated at room temperature to give orange crystalline powders. Samples for gas adsorption were subsequently evacuated at 200 °C overnight using Micromeritics Tristar flow station.

Synthesis of $[(Co_4OHsc4a)_4(BDTri)_8]^{4-}$

To a 20 mL vial, H_2BDTri (50 mg) and 6 mL of DMF were added. After the ligand had fully dissolved, dimethylformamidium trifluoromethanesulfonate (96 mg) and $CoCl_2.6H_2O$ (70

mg) was added and heated at 120 °C for 3 h. After cooling to room temperature, sc4a (100 mg) was added. Further, MeOH (2 ml) was added to the mixture and the solution was heated for an additional 48 h at 120 °C. The resultant solution was cooled to room temperature and diluted to a 2 ml EtOH solution. This mixture was heated at 120 °C until product precipitating as pink crystalline product. This solid was washed with DMF over 12 h. Subsequently, the solids were exchanged with MeOH over 2 d, with the solvent replenished with every day. MeOH was decanted and materials were evacuated at room temperature to give pink powders. Samples for gas adsorption were subsequently evacuated at 200 °C overnight using Micromeritics Tristar flow station.

X-ray structural analysis.

X-ray structural analysis for **$[(Fe_4OHsc4a)_6(BTTri)_8]^{6-}$**, **$[(Co_4OHsc4a)_6(BTTri)_8]^{6-}$**, and **$[(Co_4OHsc4a)_4(BDTri)_8]^{4-}$**: Crystals were mounted using viscous oil onto a plastic mesh and cooled to the data collection temperature. Data were collected on a D8 Venture Photon III diffractometer with Cu-Kα radiation (λ = 1.54178 Å) focused with Goebel mirrors. Unit cell parameters were obtained from fast scan data frames, 1°/s ω, of an Ewald hemisphere. The unit-cell dimensions, equivalent reflections and systematic absences in the diffraction data are consistent with *I*4, *I*-4, and *I*4/*m* for **$[(Fe_4OHsc4a)_6(BTTri)_8]^{6-}$** and **$[(Co_4OHsc4a)_6(BTTri)_8]^{6-}$**. No symmetry higher than triclinic was observed in **$[(Co_4OHsc4a)_4(BDTri)_8]^{4-}$**. Refinement in the centrosymmetric space group options yielded chemically reasonable and computationally stable results of refinement. The data were treated with multi-scan absorption corrections.[4] Structures were solved using intrinsic phasing methods[5] and refined with full-matrix, least-squares procedures on F^2.[6]

Each polyhedral structure is located at an inversion center. For **$[(Fe_4OHsc4a)_6(BTTri)_8]^{6-}$** and **$[(Co_4OHsc4a)_6(BTTri)_8]^{6-}$**, the compound molecule is located at the intersection of a mirror plane perpendicular to a four-fold axis. The disordered cell contents of highly porous metal-organic polyhedral (MOP) complexes result in diffraction data that are limited in coverage and resolution. As a result, it is common to have multiple restraints and constraints, incompletely assigned moieties, and high residuals in the structural model. Presumably disordered solvent molecules were treated as diffused contributions with identities assigned to be chemically reasonable based on the synthesis, and electron counts from the Squeeze results.[7]

Non-hydrogen atoms were refined with anisotropic displacement parameters. All hydrogen atoms were treated as idealized contributions with geometrically calculated positions and with U_{iso} equal to 1.2 U_{eq} (1.5 U_{eq} for methyl) of the attached atom. Atomic scattering factors are contained in the SHELXTL program library.[2] The structures have been deposited at the Cambridge Structural Database under the following CCDC depositary numbers: CCDC 2260661-2260663.

^{1}H-NMR Spectra

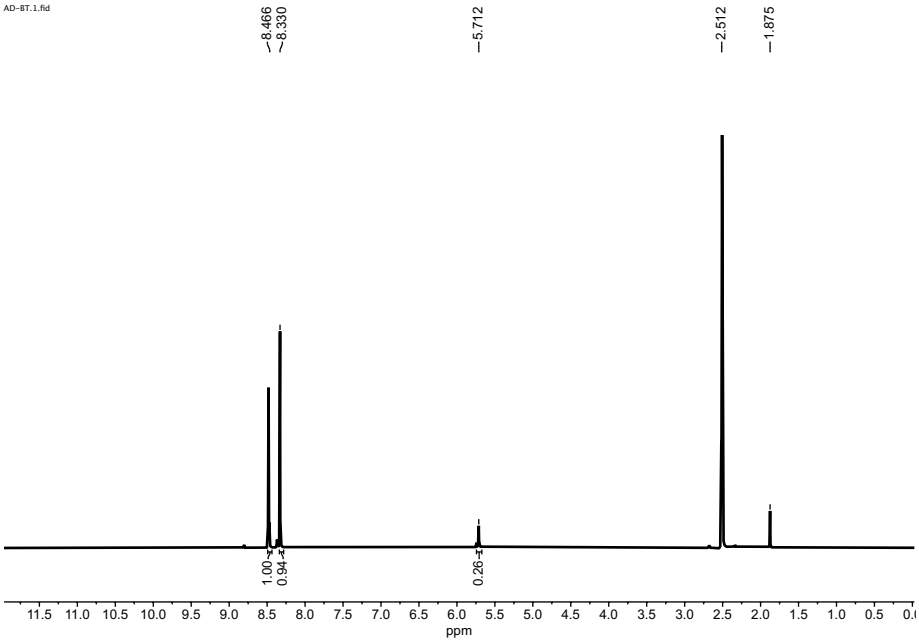

Figure S1. ^{1}H-NMR of H_3BTTri (400 MHz, DMSO-d_6): 8.466 (s, 3H), 8.33 (s, 3H), 5.712 (s, 3H).

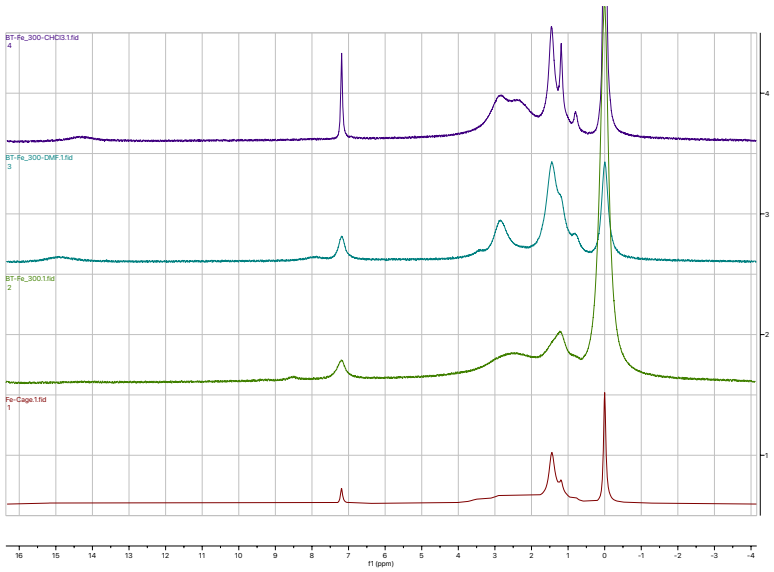

Figure S2. ^{1}H NMR (400 MHz, $CDCl_3$) of $[(Fe_4OHsc4a)_6(BTTri)_8]^{6-}$ (red), $[(Fe_4OHsc4a)_6(BTTri)_8]^{6-}$ activated at 300 °C (green), $[(Fe_4OHsc4a)_6(BTTri)_8]^{6-}$ in DMF activated at 300 °C (light blue), $[(Fe_4OHsc4a)_6(BTTri)_8]^{6-}$ in chloroform activated at 300 °C (purple).

IR Spectra

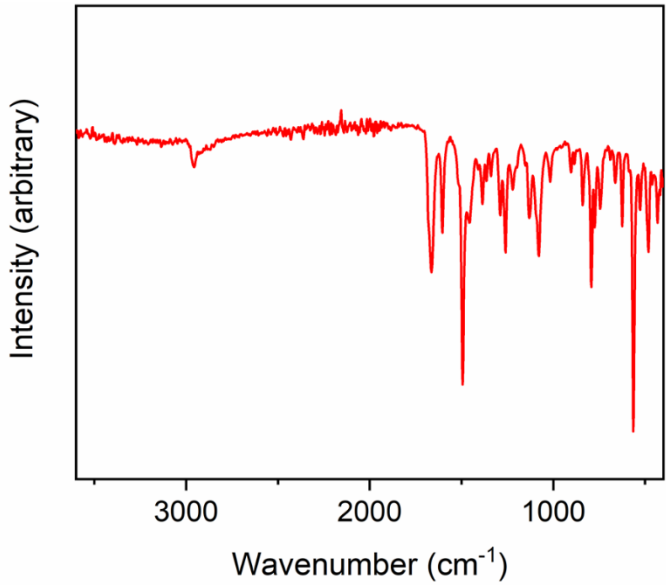

Figure S3. IR spectrum of $[(Fe_4OHsc4a)_6(BTTri)_8]^{6-}$.

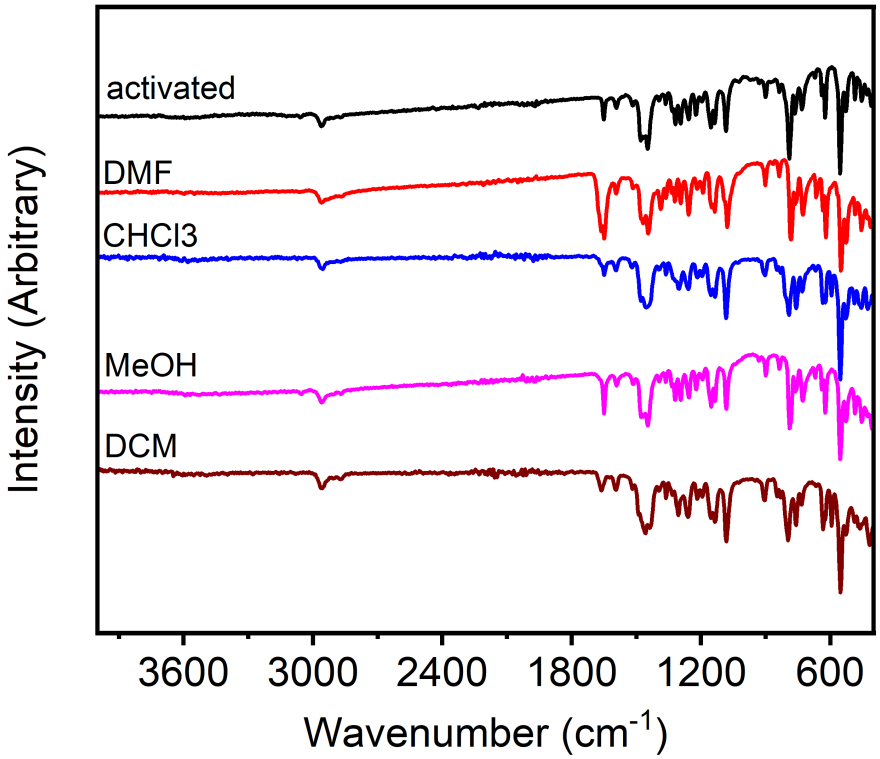

Figure S4. IR of $[(Fe_4OHsc4a)_6(BTTri)_8]^{6-}$ washed with methanol (pink), recrystallized from chloroform (blue), activated at 300 °C (black), recrystallized from chloroform after activation at 300 °C (dark red) and washed with DMF (red).

TGA

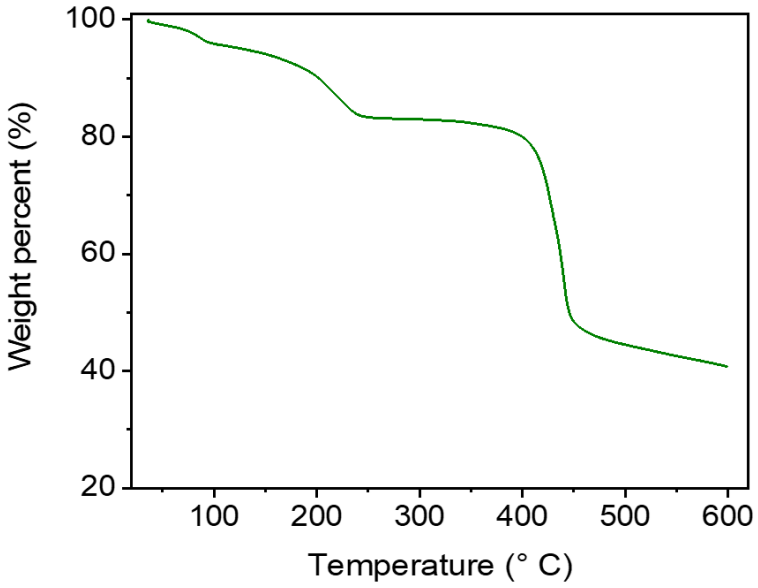

Figure S5. Thermogravimetric analysis of $[(Fe_4OHsc4a)_6(BTTri)_8]^{6-}$.

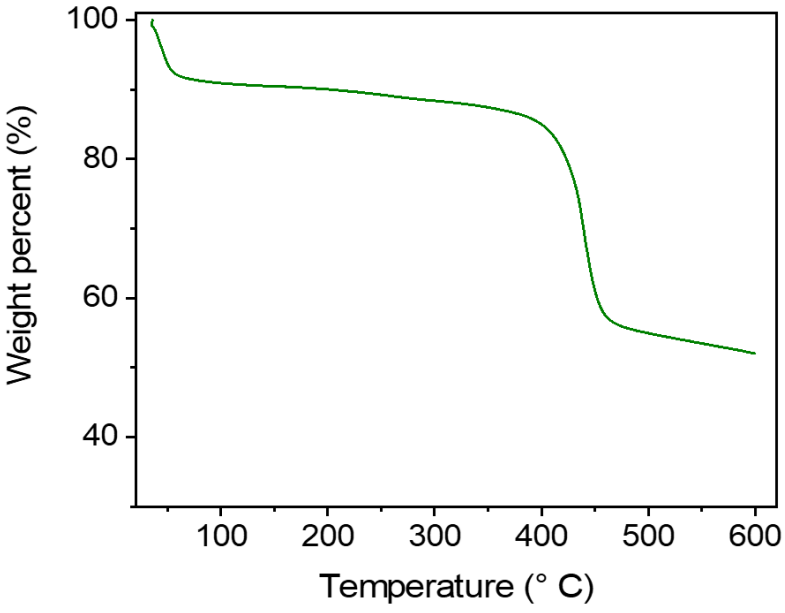

Figure S6. Thermogravimetric analysis of $[(Co_4OHsc4a)_6(BTTri)_8]^{6-}$

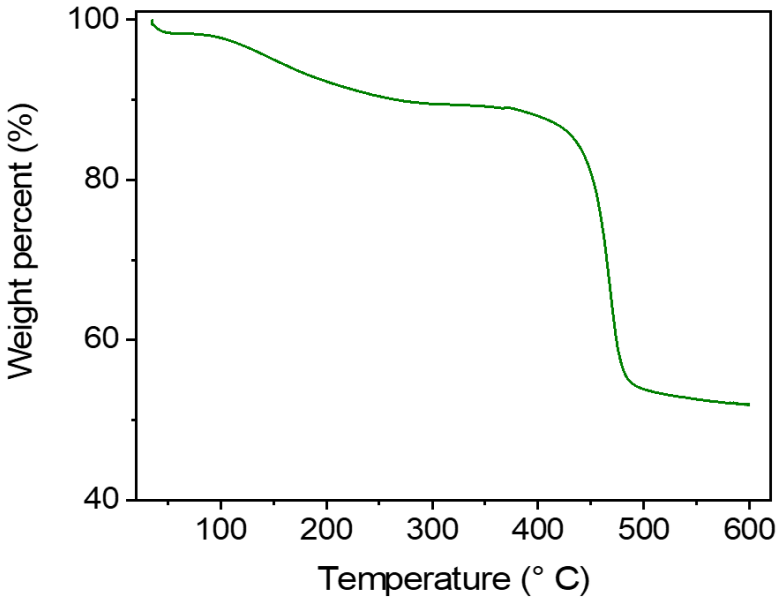

Figure S7. Thermogravimetric analysis of $[(Co_4OHsc4a)_4(BDTri)_8]^{4-}$

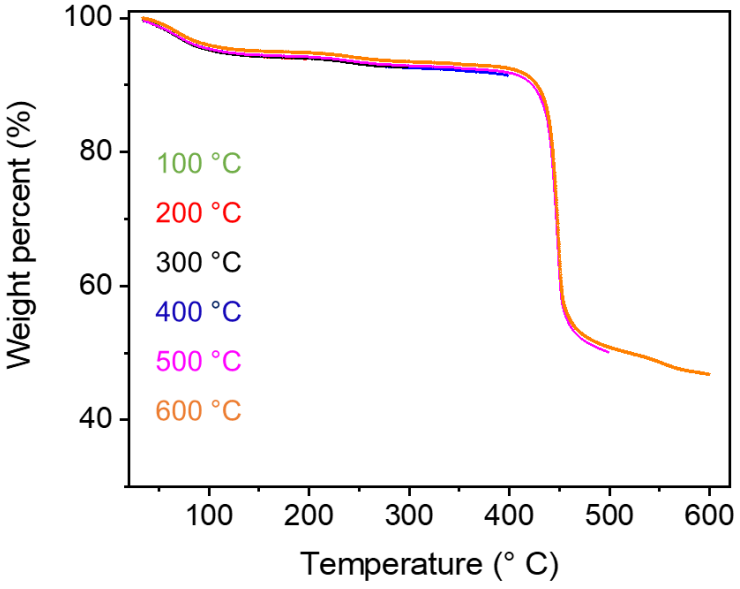

Figure S8. Thermogravimetric analysis of $[(Fe_4OHsc4a)_6(BTTri)_8]^{6-}$ up to different temperatures to determine stability as judged by IR spectroscopy (Figure 3).

Solubility Analysis and UV-Vis Spectra

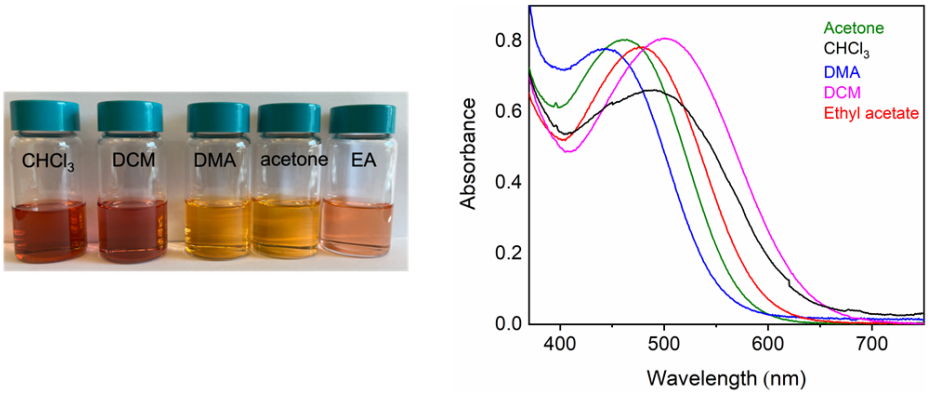

Figure S9. Solubility and UV-vis spectrum of $[(Fe_4OHsc4a)_6(BTTri)_8]^{6-}$ (1 mg in 10 mL solvent).

Table S1. Solubility chart of corresponding cages

Cage	DCM	$CHCl_3$	DMF	THF	H_2O	CH_3CN	Toluene	EtOAc	Acetone
$[(Fe_4OHsc4a)_6(BTTri)_8]^{6-}$	Y	Y	N	N	N	N	N	Y	Y
$[(Co_4OHsc4a)_6(BTTri)_8]^{6-}$	Y	Y	N	N	N	N	N	N	N
$[(Co_4OHsc4a)_4(BDTri)8]^{4-}$	N	N	N	N	N	N	N	N	N

Powder X-Ray Diffraction (PXRD) Spectra

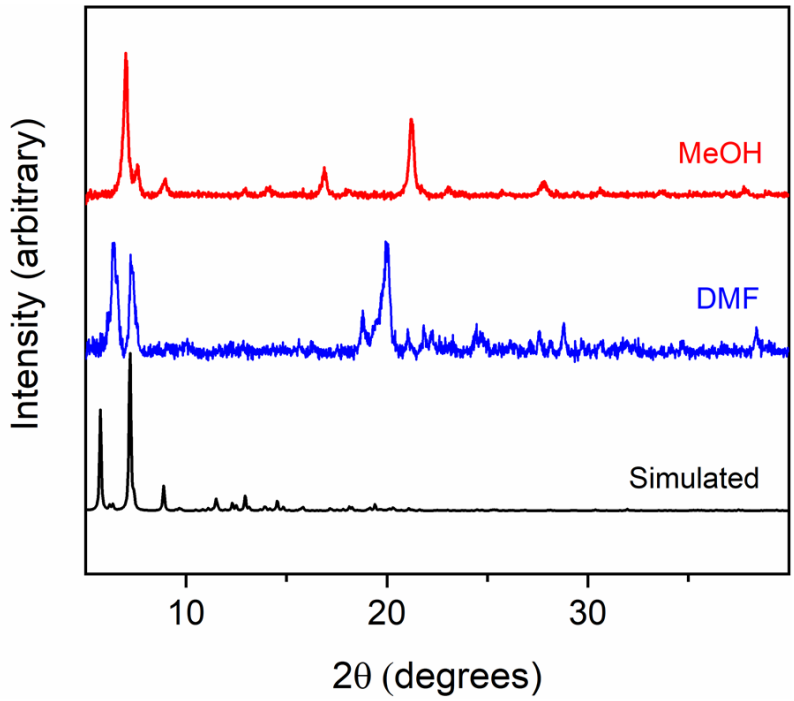

Figure S10. PXRD of $[(Fe_4OHsc4a)_6(BTTri)_8]^{6-}$.

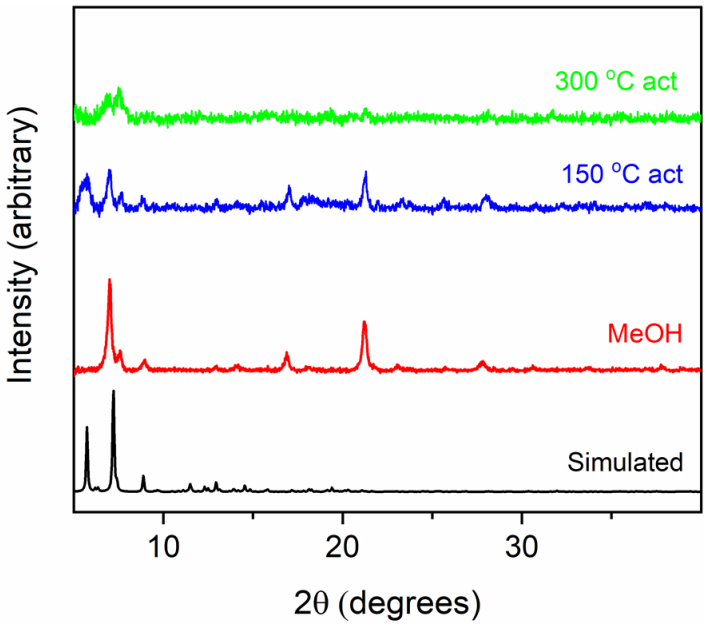

Figure S11. PXRD of $[Fe_4OHsc4a)_6(BTTri)_8]^{6-}$ upon solvent exchange and activation.

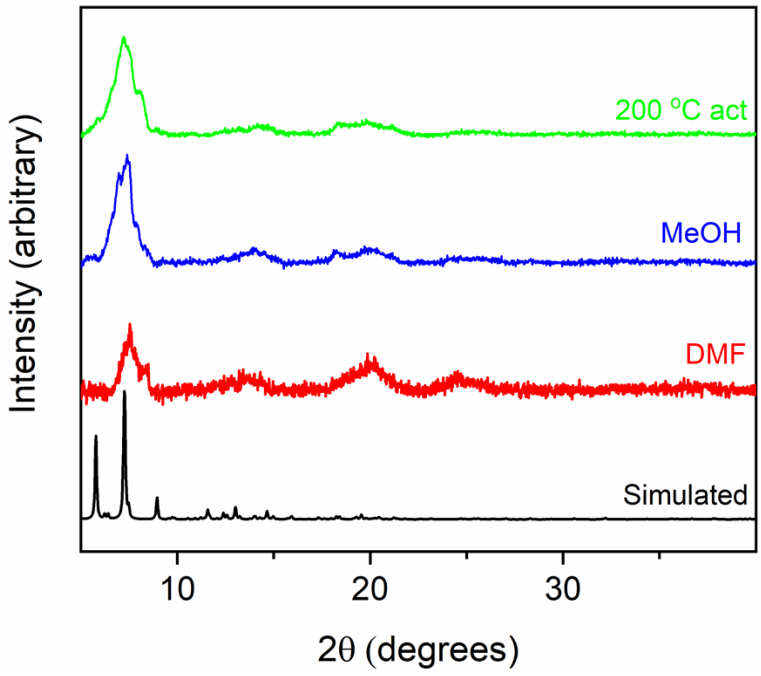

Figure S12. PXRD of $[Co_4OHsc4a)_6(BTTri)_8]^{6-}$ upon solvent exchange and activation.

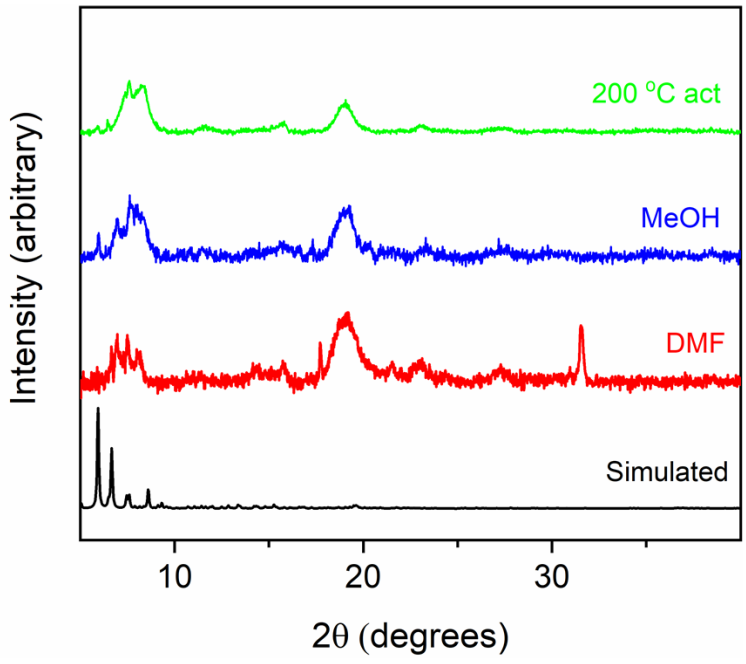

Figure S13. PXRD of $[Co_4OHsc4a)_4(BDTri)_8]^{4-}$ upon solvent exchange and activation.

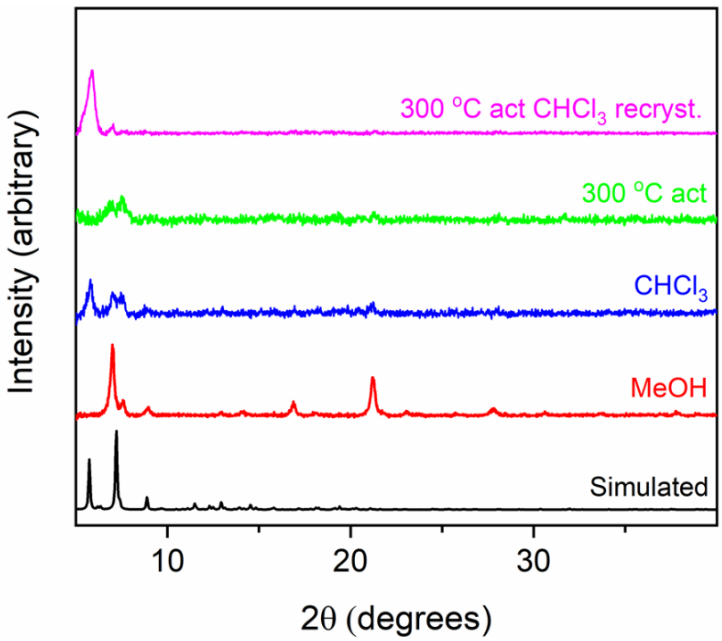

Figure S14. PXRD of $[(Fe_4OHsc4a)_6(BTTri)_8]^{6-}$ (black) simulated (red) in methanol (blue) in chloroform (green) activated at 300 °C (purple) recrystallized in chloroform and activated at 300 °C.

Mass Spectroscopy Spectra

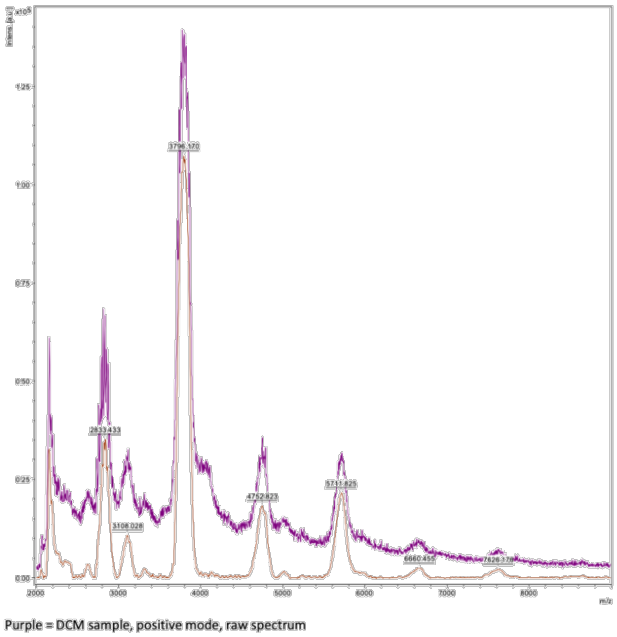

Figure S15. MALDI-TOF of the $[(Fe_4OHsc4a)_6(BTTri)_8]^{6-}$ in DCM.

Gas Adsorption Isotherms and Studies

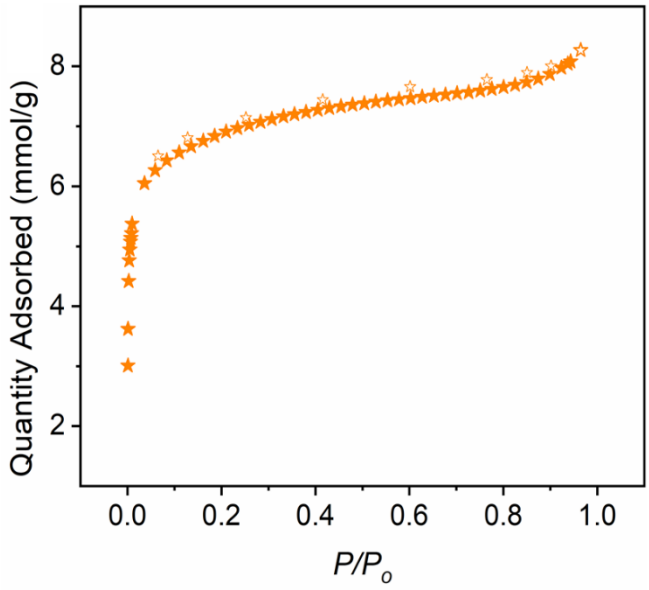

Figure S16. N_2 adsorption isotherm at 77 K for $[(Fe_4OHsc4a)_6(BTTri)_8]^{6-}$ activated at 150 °C.

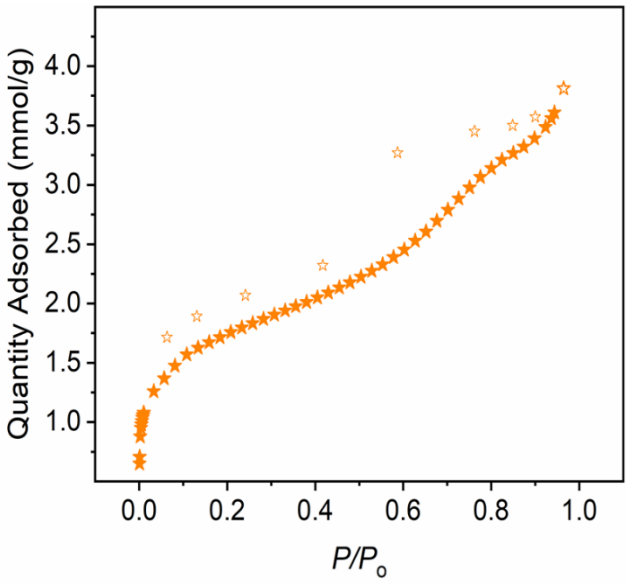

Figure S17. N_2 adsorption isotherm at 77 K for $[(Fe_4OHsc4a)_6(BTTri)_8]^{6-}$ activated at 300 °C.

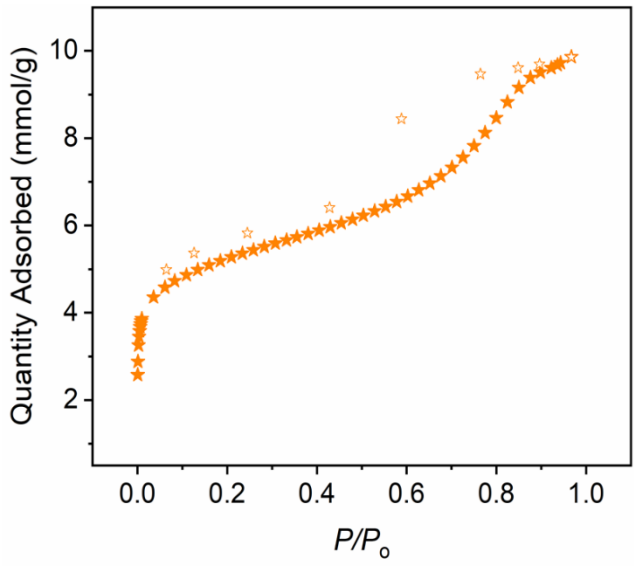

Figure S18. N_2 adsorption isotherm at 77 K for $[(Fe_4OHsc4a)_6(BTTri)_8]^{6-}$ washed with methanol and activated at 150 °C.

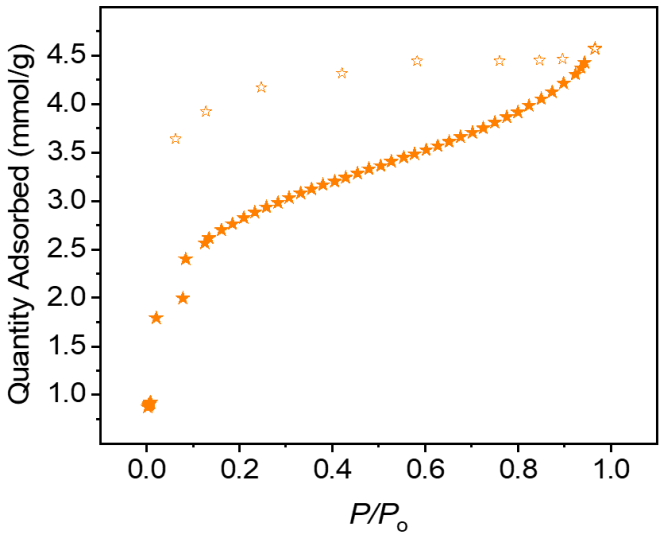

Figure S19. N_2 adsorption isotherm at 77 K for $[(Fe_4OHsc4a)_6(BTTri)_8]^{6-}$ recrystallized in chloroform and activated at 150 °C.

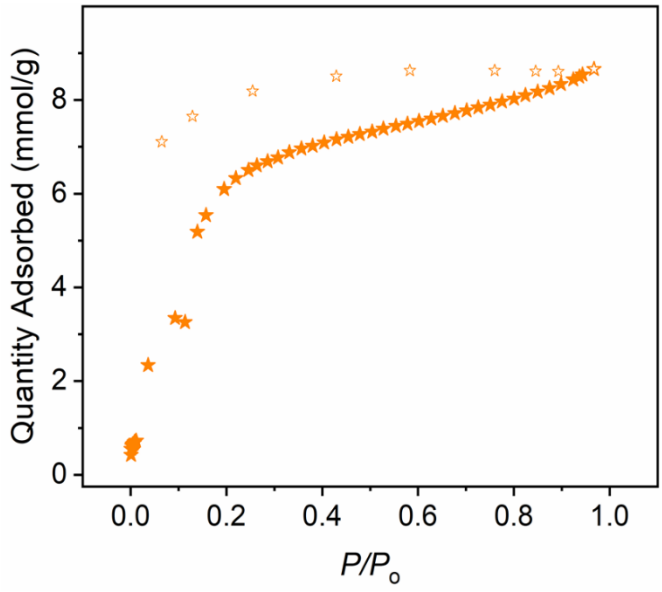

Figure S20. N_2 adsorption isotherm at 77 K for $[(Fe_4OHsc4a)_6(BTTri)_8]^{6-}$ activated at 300 °C, recrystallized in chloroform, and re-activated at 150 °C.

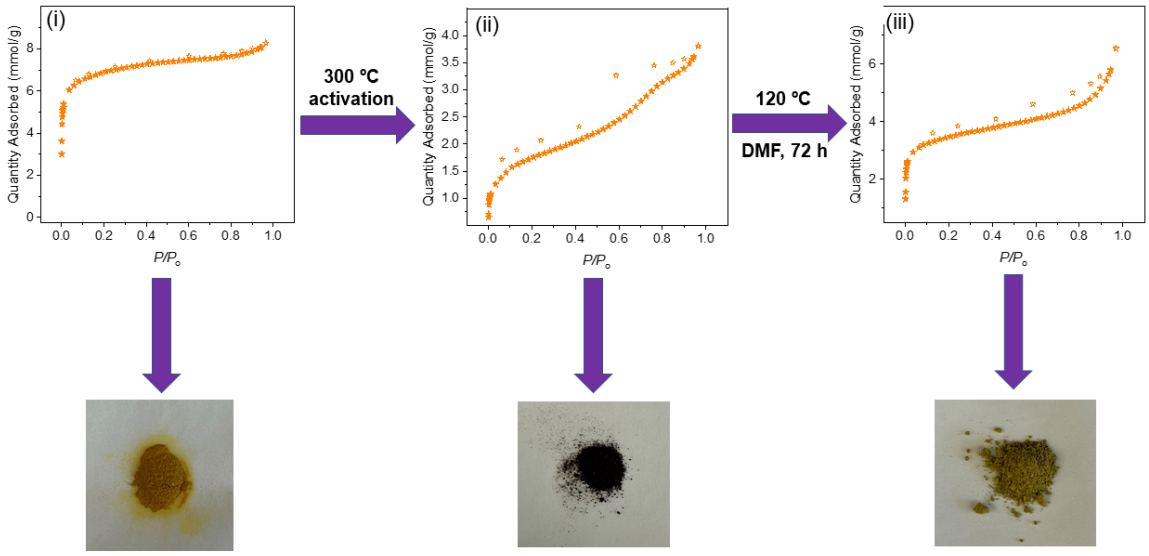

Figure S21. Regeneration of $[(Fe_4OHsc4a)_6(BTTri)_8]^{6-}$ from nonporous state to parent porous phase again.

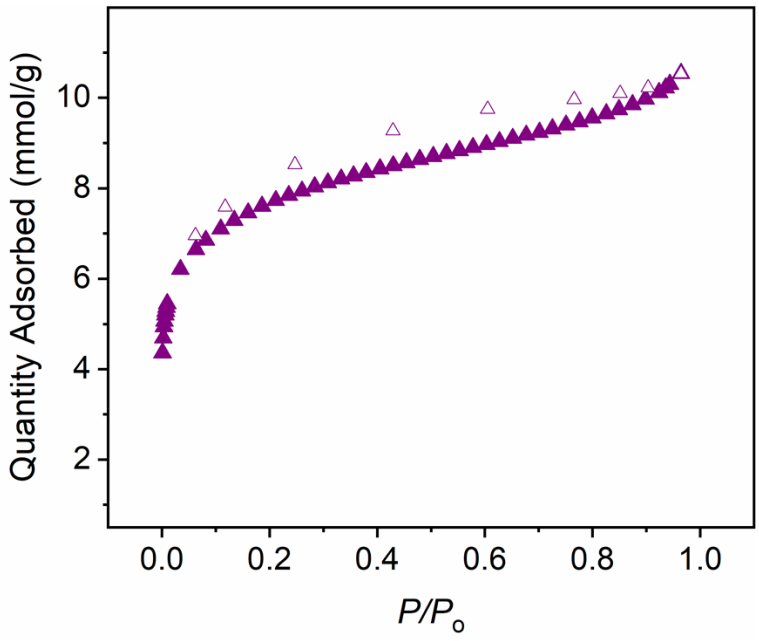

Figure S22. N_2 adsorption isotherm at 77 K for $[(Co_4OHsc4a)_6(BTTri)_8]^{6-}$ activated at 200°C

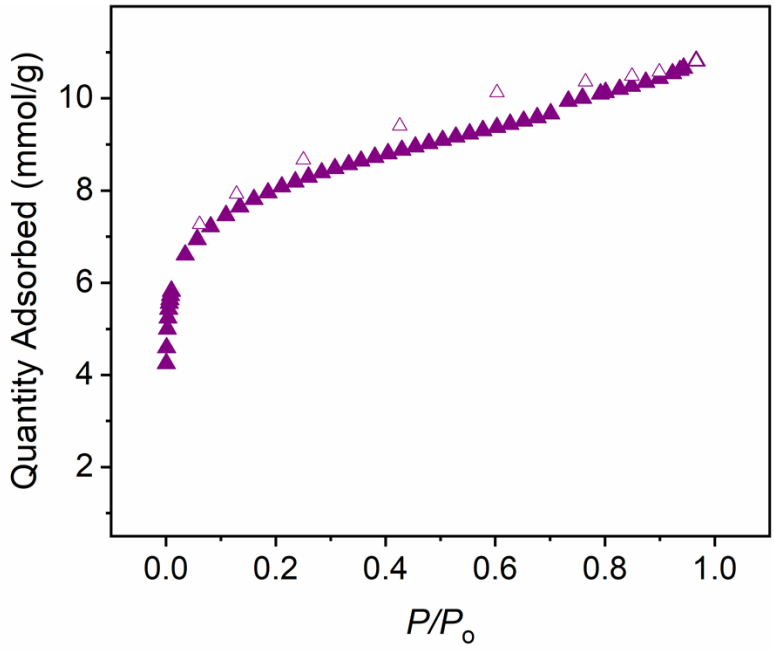

Figure S23. N_2 adsorption isotherm at 77 K for $[(Co_4OHsc4a)_6(BTTri)_8]^{6-}$ activated at 300 °C.

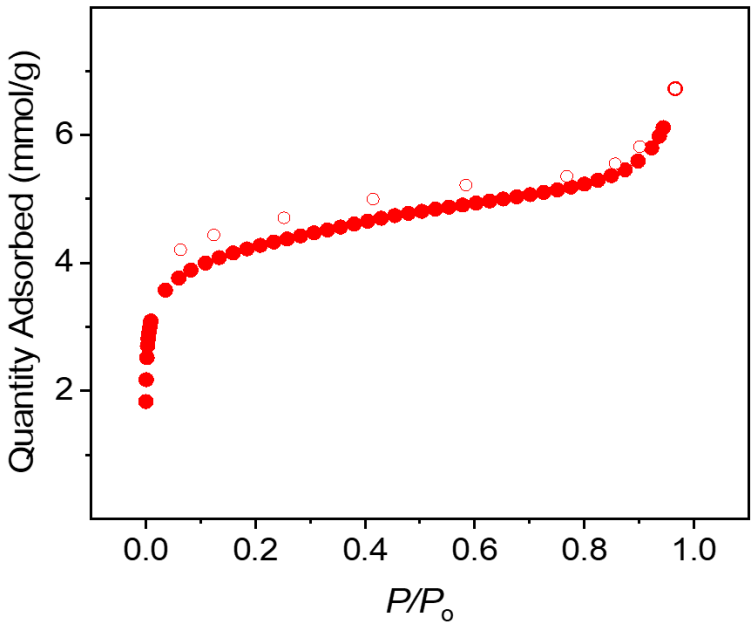

Figure S24. N_2 adsorption isotherm at 77 K for $[(Co_4OHsc4a)_4(BDTri)_8]^{4-}$ activated at 200 °C.

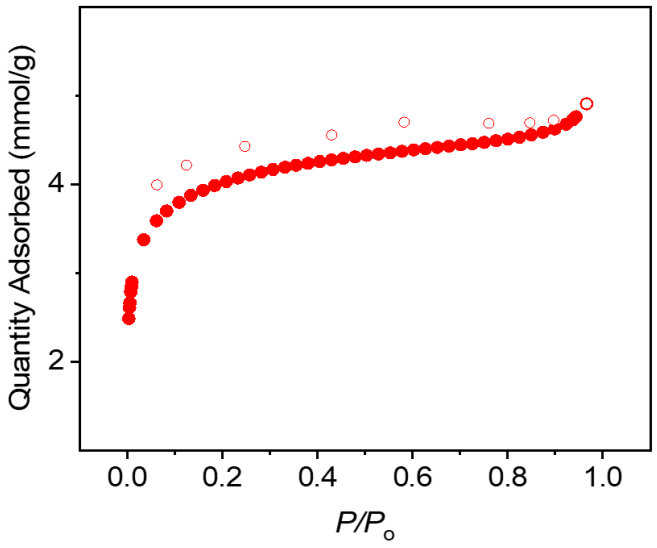

Figure S25. N_2 adsorption isotherm at 77 K for $[(Co_4OHsc4a)_4(BDTri)_8]^{4-}$ activated at 300 °C.

Table S2. Experimental surface areas of coordination cages after 150 °C activation.

Cage	N_2 BET(Langmuir) Surface Area (m^2/g)	CO_2 BET(Langmuir) Surface Area (m^2/g)	H_2 Adsorbed (mmol/g)	CH_4 Adsorbed (mmol/g)
$[(Fe_4OHsc4a)_6(BTTri)_8]^{6-}$	488(858)	468(785)	2.52	2.95
$[(Co_4OHsc4a)_6(BTTri)_8]^{6-}$	559(1067)	502(1086)	3.4	2.74
$[(Co_4OHsc4a)_4(BDTri)8]^{4-}$	307(616)	341(564)	2.12	1.98

Table S3. N_2 Langmuir surface areas of $[(Fe_4OHsc4a)_6(BTTri)_8]^6$ after recrystallization from different solvents and varying activation temperatures.

Recrystallization/Activation Conditions	N_2 BET(Langmuir) Surface Area (m^2/g)
150 °C activated	488(858)
200 °C activated	(689)
250 °C activated	(634)
300 °C activated	(432)
400 °C activated	(389)
$CHCl_3$ recrystallized, 150 °C activated	215(536)
$CHCl_3$ recrystallized, 300 °C activated	132(468)
300 °C activated, $CHCl_3$ recrystallized, 150 °C activated	625(928)
acetone recrystallized 150 °C activated	(278)
ethyl acetate recrystallized 150 °C activated	(270)
DCM recrystallized 150 °C activated	(161)

Scanning Electron Microscopy (SEM) Images

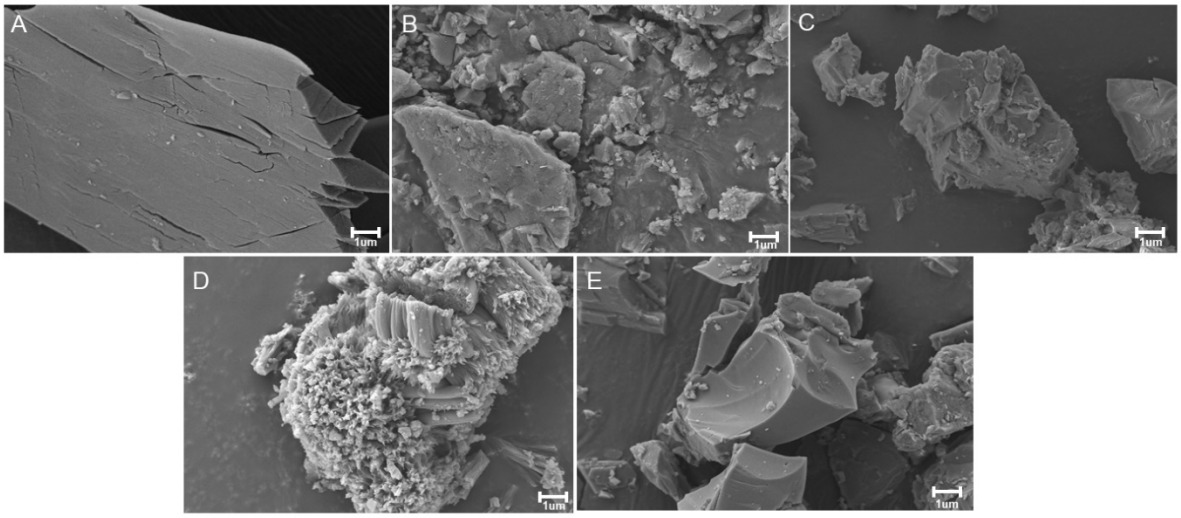

Figure S26. SEM images of the (A) $[(Fe_4OHsc4a)_6(BTTri)_8]^{6-}$ (B) activated at 300 °C (C) recrystallized in methanol and activated at 300 °C (D) recrystallized in chloroform (E) recrystallized in chloroform and activated at 300 °C.

X-Ray Photoelectron Spectroscopy (XPS) Spectra

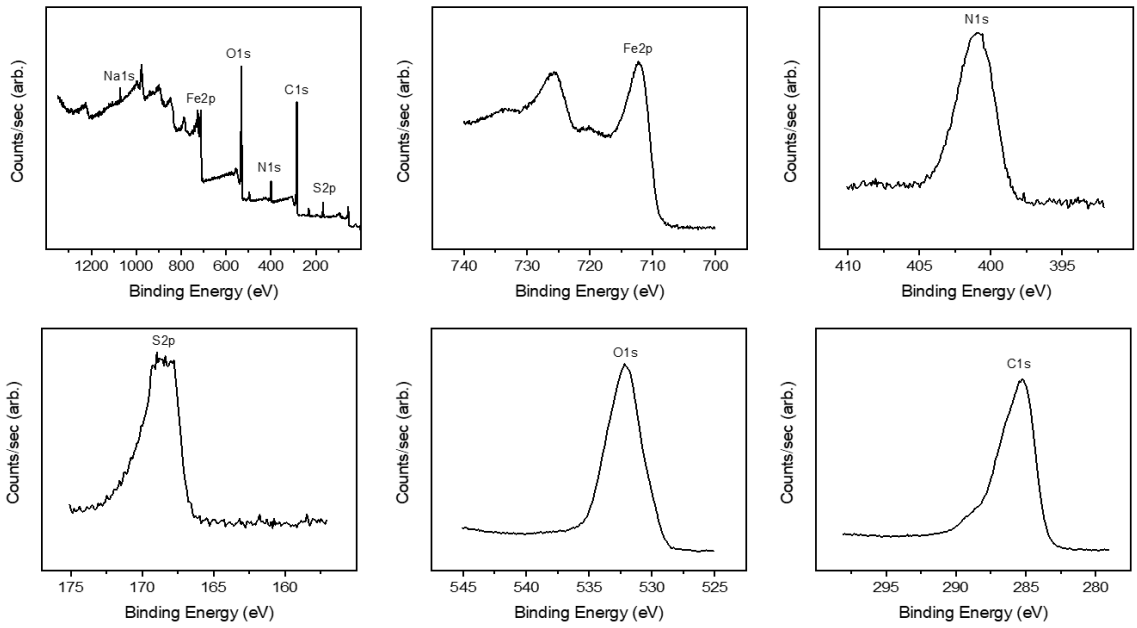

Figure S27. XPS survey spectrum (top right) and high-resolution XPS spectra of Fe (top middle), N (top left), S (bottom left), O (bottom middle), C (bottom left) of $[(Fe_4OHsc4a)_6(BTTri)_8]^{6-}$.

Detailed Crystallographic Depictions and Information

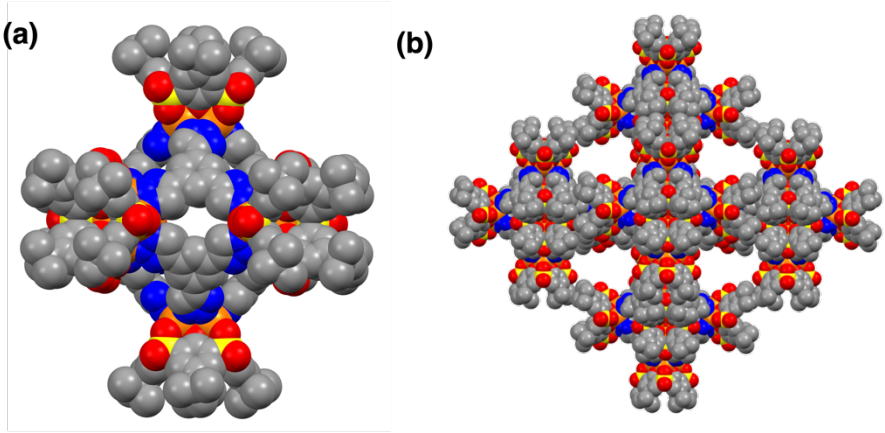

Figure S28. (a) Solid-state structure of octahedral cage $[(Fe_4OHsc4a)_6(BTTri)_8]^{6-}$ in space filling model. (b) Cage-cage interactions are governed by the tert-butyl groups on the cluster (b-axis).

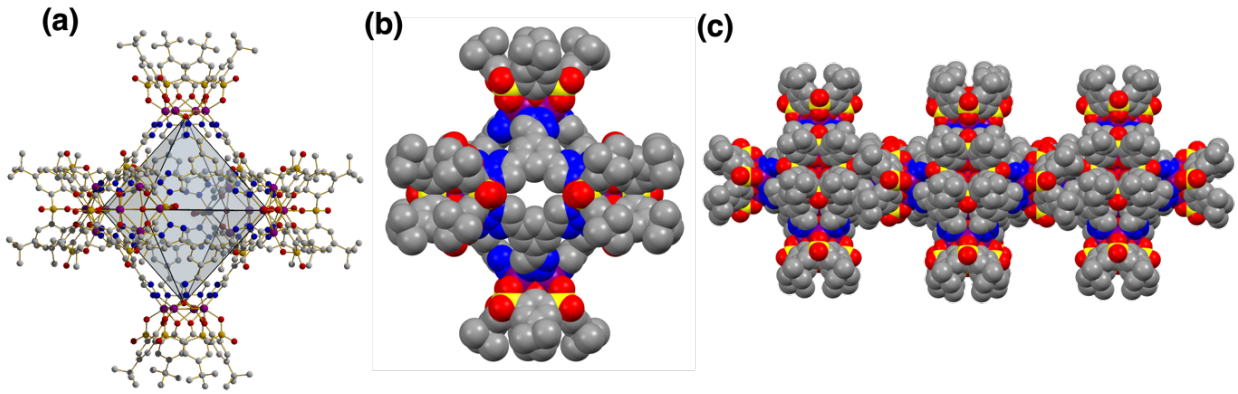

Figure S29. (a) Solid-state structure of octahedral cage $[(Co_4OHsc4a)_6(BTTri)_8]^{6-}$) (isostructural with $[(Fe_4OHsc4a)_6(BTTri)_8]^{6-}$) (b) Structure of octahedral cage of $[(Co_4OHsc4a)_6(BTTri)_8]^{6-}$ in space filling model. (c) Cage-cage interactions are governed by the tert-butyl groups on the cluster (b-axis).

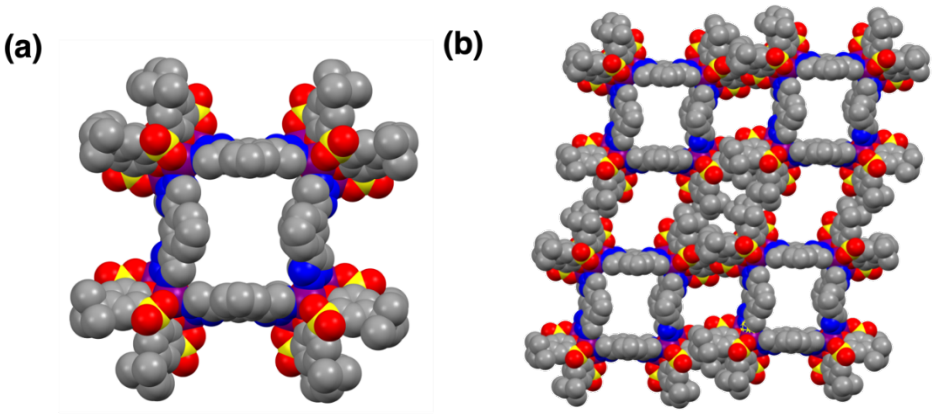

Figure S30. (a) Solid-state structure of truncated octahedral cage of $[(Co_4OHsc4a)_4(BDTri)_8]^{4-}$ in space filling model. (b) Cage-cage interactions are governed by the tert-butyl groups on the cluster (a-axis).

Table S4. Crystal data and structure refinement details.

Compound	$[(Fe_4OHsc4a)_6(BTTri)_8]^{6-}$	$[(Co_4OHsc4a)_6(BTTri)_8]^{6-}$	$[(Co_4OHsc4a)_4(BDTri)_8]^{4-}$
Sum Formula	$C_{600}Fe_{24}H_{928}N_{160}O_{166}S_{24}$	$C_{348}Co_{24}H_{1032}N_{176}O_{182}S_{24}$	$C_{336}Co_{16}H_{462}N_{78}O_{88}S_{16}$
Moiety Formula	$C_{336}H_{312}F_{24}N_{72}O_{78}S_{24}$, $88[C_3H_7NO]$	$C_{336}H_{304}Co_{24}N_{72}O_{78}S_{24}$, $104[C_3H_7NO]$	$C_{240}H_{228}Co_{16}N_{48}O_{52}S_{16}$, $2(C_3H_7NO)$, $28[C_3H_7NO]$, $6[CH_3OH]$
Formula Weight, g/mol	15148.81	16384.19	8457.65
Temperature, K	120.0	100.0	100.0
Crystal system	tetragonal	tetragonal	triclinic
Space group	*I*4/*m*	*I*4/*m*	*P*-1
Cell dimensions			
a, Å	28.4778(18)	28.324(2)	12.3693(10)
b, Å	28.4778(18)	28.324(2)	27.890(2)
c, Å	47.719(3)	47.231(6)	31.192(2)
α, °	90	90	104.673(4)
β, °	90	90	97.371(4)
γ, °	90	90	98.450(5)
Volume, $Å^3$	38700(6)	37891(8)	10141.4(13)
Z	2	2	1
ρ_{calc}, g/cm^3	1.300	1.436	1.385
μ/mm^{-1}	4.775	5.371	6.436
F(000)	15968.0	17280.0	4416.0
Reflections collected	45069	75827	79460
Independent reflections	10343	12313	20236
Data/restraints/parameters	10337/599/581	12313/605/580	20236/3405/1696
Goodness-of-fit	1.076	1.237	1.034
R [I>=2σ (I)] R_1/wR_2	0.1070/0.3049	0.1160/0.3130	0.1014/0.2713
R indexes [all data] R_1/wR_2	0.1609/0.3359	0.1672/0.3541	0.1438/0.3079
CCDC	2260661	2260662	2260663

Table S5.

cage	geometry	μ_4 OH-OH/Cl-Cl cross cage (Å)	μ_4 OH-OH/Cl-Cl adjacent/nearest cluster(Å)	Metal to closest triazole N /carboxyl O in ligand (Å)	Metal to closest S in cap (Å)	Metal to closest sulfonyl O in cap	Metal to closest phenolic O in cap	Metal to triazole C attached to benzene/carboxyl C in the ligand. (Å)	Metal to Closest C in benzene ring of ligand
Fe-SC4A-Tritopic linker	Octahedral	13.089(Cl-Cl)	9.277(Cl-Cl)	2.035	3.087	2.085	2.124	2.991	4.349
Co-Sc4A-Tritopic Linker	Octahedral	13.574	9.598	2.012	3.082	2.099	2.085	2.945	4.312
Co-Sc4A-Bent ditopic linker	Box-like	13.678	9.895	2.022	3.088	2.102	2.075	2.969	4.302
$[(Fe_4OHsc4a)_6(BTTri)_8]^{6-}$	Octahedral	17.837	12.584	2.072	3.139	2.056	2.128	4.222	5.649
$[(Co_4OHsc4a)_6(BTTri)_8]^{6-}$	Octahedral	17.589	12.429	2.043	3.103	2.091	2.090	4.206	5.639
$[(Co_4OHsc4a)_4(BDTri)_8]^{4-}$	Truncated octahedral	17.010	12.505	2.045	3.122	2.105	2.108	4.199	5.554
Fe-SC4A-Tatb	Octahedral	23.138(Cl-Cl)	16.267(Cl-Cl)	2.09	2.941	2.04	2.05	4.381	4.295

References

(1) Kumagi, H.; Hasegawa, M.; Miyanari, S.; Sugawa, Y.; Soto, Y.; Hori, T.; Ueda, S.; Kamiyama, H.; Miyano, S. *Tetrahedron Lett.* **1997**, *38*, 3971-3972.
(2) Iki, N.; Kumagai, H.; Morohashi, N.; Eijma, K.; Hasegawa, M.; Miyanari, S.; Miyano, S. *Tetrahedron Lett.* **1998**, *39*, 7559-7562.
(3) Xiao, D. J.; Gonzalez, M. I.; Darago, L. E.; Vogiatzis, K. D.; Haldoupis, E.; Gagliardi, L.; Long, J. R. *J. Am. Chem. Soc.* **2016**, *138*, 7161-7170.
(4) Apex4 [Computer Software]; Bruker AXS Inc.: Madison, WI, USA, 2021.
(5) Sheldrick, G.M. Acta Cryst. **2015**, *A71*, 3–8.
(6) Sheldrick, G.M. *Acta Cryst.* **2015**, *C71*, 3–8.
(7) Spek, A. L. *Acta Cryst.* **2015**, *C71*, 9–18.